Pediatr Radiol (2012) 42:1490–1501
DOI 10.1007/s00247-012-2495-y

PICTORIAL ESSAY

Osteoid osteomas: a pain in the night diagnosis

Nancy Laurence · Monica Epelman · Richard I. Markowitz · Camilo Jaimes · Diego Jaramillo · Nancy A. Chauvin

Received: 31 May 2012 / Revised: 1 August 2012 / Accepted: 2 August 2012 / Published online: 23 October 2012

Abstract Osteoid osteoma is a common benign bone-forming lesion that is composed of a nidus of vascular osteoid tissue and woven bone lined by osteoblasts. It is frequently associated with considerable surrounding inflammation. The diagnosis is usually straightforward when imaging reveals a radiolucent nidus surrounded by variable degrees of reactive sclerosis. However, the diagnosis can be elusive when osteoid osteomas occur in atypical locations, as they may have a nonspecific and misleading appearance on different imaging modalities, particularly on MRI. The purpose of this pictorial essay is to review the typical and atypical features of osteoid osteomas on different imaging modalities, and the appearance of osteoid osteomas in different locations. We also review growth disturbances caused by osteoid osteomas and potential mimickers, with imaging characteristics that can aid in diagnosis.

Keywords Neoplasms · Bone tissue · Osteoid osteoma · Imaging · Children

CME activity This article has been selected as the CME activity for the current month. Please visit the SPR Web site at www.pedrad.org on the Education page and follow the instructions to complete this CME activity.

Disclosure The authors listed below have indicated they have no relevant financial relationships or potential conflicts of interest related to the material.

N. Laurence · M. Epelman · R. I. Markowitz · C. Jaimes · D. Jaramillo · N. A. Chauvin (✉)
Department of Radiology, The Children's Hospital of Philadelphia, Perelman School of Medicine at the University of Pennsylvania, 34th St. and Civic Center Blvd., Philadelphia, PA 19104, USA
e-mail: chauvinn@email.chop.edu

M. Epelman
Department of Radiology, Nemours Children's Hospital, 13535 Nemours Parkway, Orlando, FL 32827, USA

Introduction

In 1935, Jaffe [1] coined the term osteoid osteoma. Osteoid osteoma is the most common benign bone-forming lesion, comprising approximately 12% of benign bone tumors [2, 3]. It is the third-most-common benign bone neoplasm after osteochondroma and nonossifying fibroma. Osteoid osteomas are much more frequent in boys, and usually present between ages 7 and 25 [3, 4]. The classic presentation is of pain that is worse at night and ameliorated by nonsteroidal anti-inflammatory drugs (NSAIDs). Although pain is often referred to a nearby joint, it may be so distant from the lesion that radiographic examinations are misdirected. Localized tenderness to touch and pressure and local swelling might be present, particularly when the bone involved is in close proximity to the skin [5]. Much of this swelling may be secondary to the highly vascular nature of the tumor, which can be confirmed by angiography, scintigraphy, Doppler sonography and MRI [6–10]. This may also be mediated by the production of prostaglandins, which can affect soft tissue and vascular permeability. Prostaglandin levels in the nidus are 100–1,000 times that of normal bone and are thought to be important in the perception of pain [11]. The pain relief associated with NSAIDs has also been attributed to the inhibition of this prostaglandin production [12]. Intra-articular prostaglandins are thought to be responsible for the related lymphofollicular synovitis [13]. Prostaglandins are also believed to lead to vasodilatation and edema in the surrounding medullary tissues, reflected as hyperintense areas on T2-weighted sequences on MRI [14–16]. Depending on the location of the lesion, other less common presentations include swelling, limp, growth disturbance, painful scoliosis, joint stiffness or contracture [3]. Painless presentations are also recognized, particularly those involving the phalanges of the hands and feet [17, 18].

Osteoid osteomas are composed of a nidus of vascular osteoid tissue and woven bone lined by osteoblasts. Even

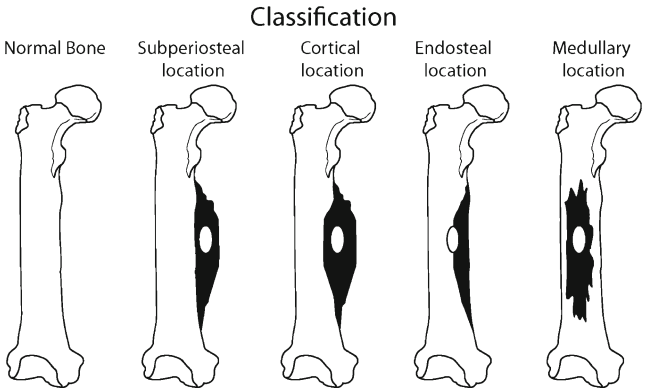

Fig. 1 Location of osteoid osteomas in tubular bones (adapted from Kayser et al. [24]). The nidus is depicted in white. Black areas show sclerosis, new bone formation or edema

though there may be considerable inflammation associated with osteoid osteomas, the tumor itself (nidus) rarely exceeds 1.5 cm. The precise location of the nidus must be determined, since its removal is necessary for cure [2]. The pathogenesis of this lesion is controversial. While some authors believe it to be a benign neoplasm, others believe it may represent an unusual healing process or arise on an inflammatory basis [19, 20]. Whether osteoid osteomas are a true neoplasm is also questioned because its growth potential is limited. There is no known malignant potential.

With special immunohistochemical techniques, abundant nerve fibers can be demonstrated within the nidus and particularly within the adjacent zone of sclerosis [21, 22].

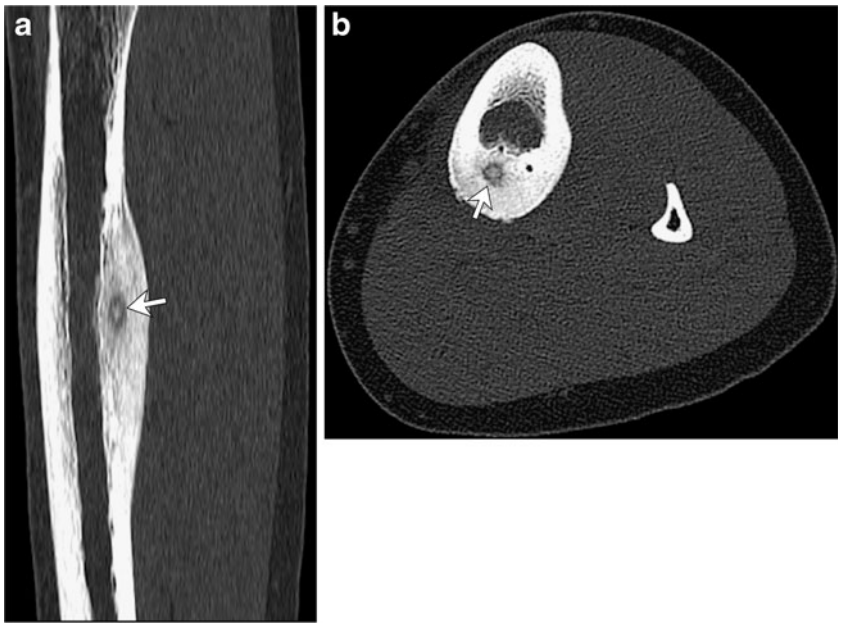

Fig. 2 Cortical osteoid osteoma in a 14-year-old boy with 8 weeks of tibial pain. Sagittal (**a**) and axial (**b**) CT images show a radiolucent nidus with central calcification (*arrows*) and surrounding fusiform cortical thickening

Fig. 3 Cortical osteoid osteoma in a 4-year-old boy with right hip pain. **a** Coronal STIR MR image shows the fusiform shape of the hyperintense nidus in the medial cortex (*arrow*) and the extent of bone marrow edema in the proximal femur. Axial precontrast (**b**) and postcontrast (**c**) fat-saturated T1-weighted MR images show intense enhancement of the nidus (*arrow*) and mild enhancement of the bone marrow and soft-tissue edema

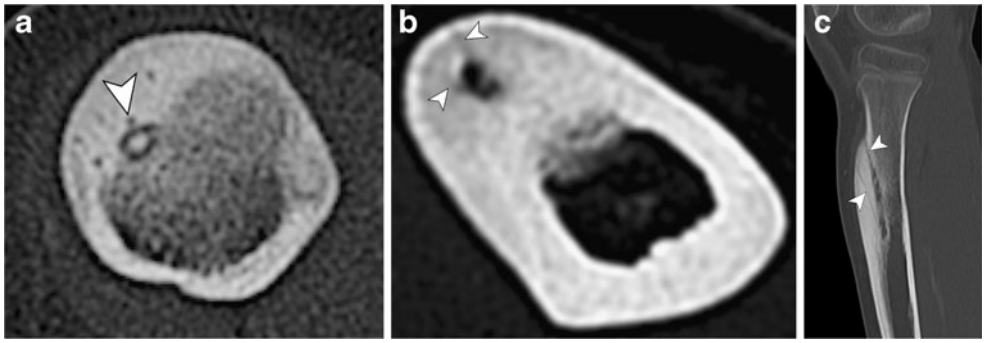

Fig. 4 "CT vessel" also known as "vascular groove" sign in two patients. **a** Axial CT image of the right tibia in a 14-year-old boy shows a linear low-density groove (*arrowhead*) entering the centrally calcified nidus. Axial (**b**) and sagittal reformatted (**c**) images of the left tibia in a 7-year-old girl demonstrate linear vascular grooves (*arrowheads*) coursing toward an elongated low-density nidus in the anterior tibial cortex

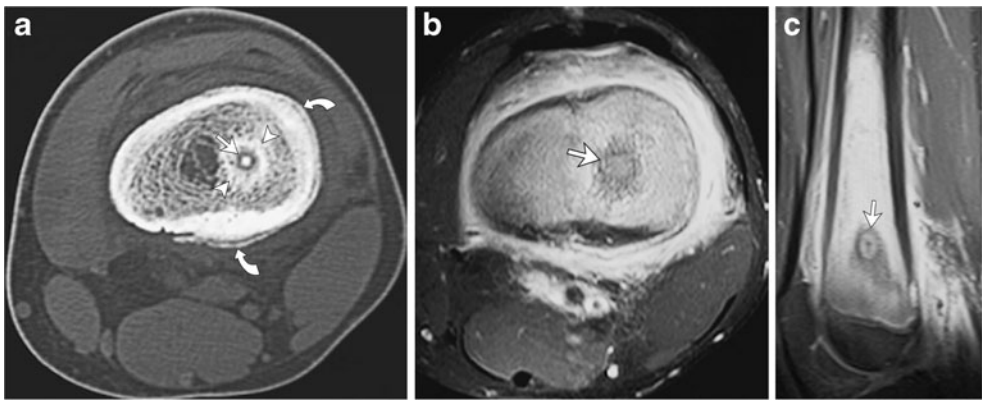

Fig. 5 Intramedullary metadiaphyseal left femoral osteoid osteoma in a 17-year-old boy. **a** Axial CT image demonstrates periosteal reaction (*curved arrows*) along the posterolateral aspect of the femur. Calcification is noted within the nidus (*arrowhead*) and surrounding reactive sclerosis (*arrowheads*). Axial (**b**) and sagittal (**c**) fat-saturated T1-weighted MR images post contrast show enhancement of the nidus (*arrows*) and a central dot of hypointense calcification. A hypointense rim surrounds the nidus consistent with sclerosis. Reactive periosteal reaction, mild synovitis and effusion are noted as well

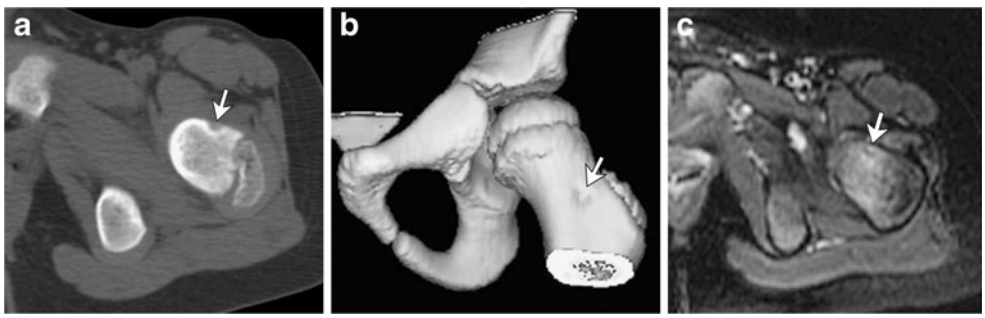

Fig. 6 Subperiosteal osteoid osteoma in a 6-year-old boy with left hip pain. **a** Axial CT image through the center of the nidus demonstrates the subperiosteal location of the radiolucent nidus (*arrow*) with a tiny central dot of calcification. **b** Reformatted 3-D CT image demonstrates the excavation (*arrow*) of the femoral cortex exerted by the nidus. **c** Axial fat-saturated T2-weighted MR image of the left hip shows bone marrow edema within the left femoral metaphysis, and a rounded relatively well-defined area of high signal in a subperiosteal location with a surrounding hypointense rim, consistent with an osteoid osteoma nidus (*arrow*)

Fig. 7 Subperiosteal intra-articular osteoid osteoma in a 10-year-old boy with left hip pain. **a** Coronal STIR MR image shows focal bone marrow edema in the left femoral neck (*arrowheads*) and a small joint effusion (*asterisk*). **b** Coronal fat-saturated T1-weighted post-contrast MR image demonstrates synovial thickening and enhancement (*curved arrows*) around a joint effusion (*asterisk*). **c** Subsequent axial CT image shows a subperiosteal partially calcified nidus (*arrow*). **d** In retrospect, the subperiosteal nidus (*arrow*) was visible on this axial fat-saturated T2-weighted MR image with a surrounding hypointense rim of sclerosis

These nerve fibers belong to the osseous nerve supply, which plays an important role in skeletal development and homeostasis. Large amounts of nerve fibers have been encountered in healing fractures as well. It is believed that nerve fibers proliferate to provide information about the fracture site and that they might also be actively involved in bone formation and remodeling by the exertion of a paracrine effect on osteoblasts through the production and release of cytokines, such as calcitonin gene-related peptide [23]. It is possible that the same mechanism applies with

Fig. 8 Intra-articular osteoid osteoma in a 9-year-old boy with elbow pain. Axial (**a**) and coronal (**b**) CT images of the elbow show a subtle lucent nidus (*arrows*) in the olecranon fossa with no reactive sclerosis, initially overlooked. **c** Sagittal T2-weighted MR image shows the nidus (*arrows*) with a hypointense rim. **d** Coronal fat-saturated T2-weighted MR image shows hyperintense bone marrow edema in the distal humerus (*arrowheads*) adjacent to the rounded nidus (*arrows*), which has a T2 hypointense rim

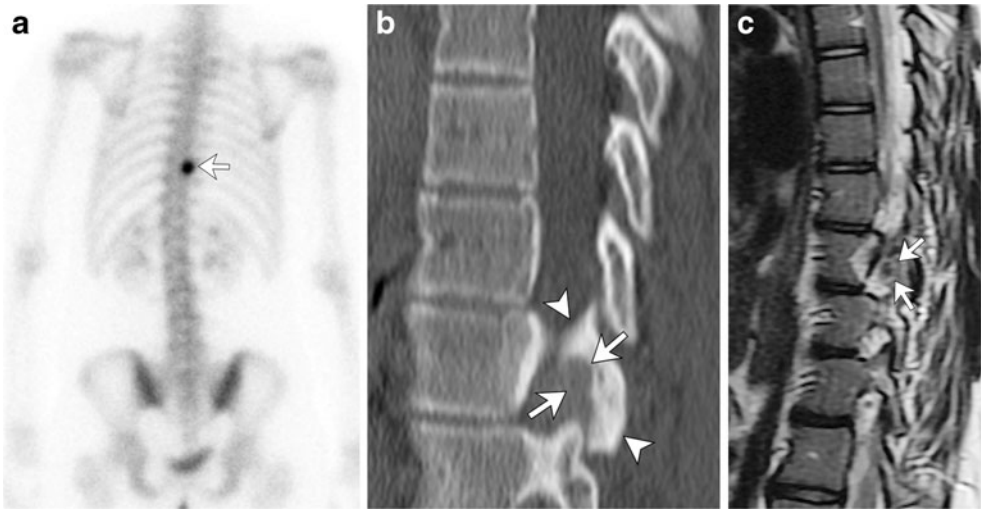

Fig. 9 Spinal osteoid osteoma in a 14-year-old girl with mid back pain. **a** Posterior image from a whole-body bone scan shows focal uptake in the right T9 pedicle (*arrow*) and mild antalgic levocurvature of the spine. **b** Sagittal CT reformation shows a lucent nidus in the right pedicle (*arrows*) and surrounding sclerosis (*arrowheads*). **c** Sagittal T2-weighted MR image shows the rounded nidus (*arrows*) with a posterior hypointense rim of sclerosis

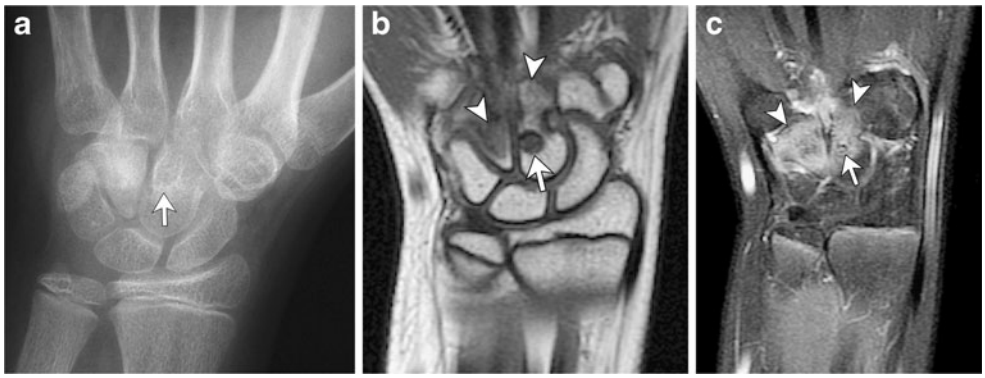

Fig. 10 Osteoid osteoma of the capitate in a 14-year-old girl with 3 years of wrist pain and swelling. **a** AP radiograph of the wrist shows subtle focal sclerosis with central lucency in the capitate (*arrow*). Coronal T1-weighted (**b**) and coronal fat-saturated postcontrast T1-weighted (**c**) MR images demonstrate a T1 hypointense rounded nidus (*arrows*) and adjacent enhancing edema in the capitate and hamate (*arrowheads*)

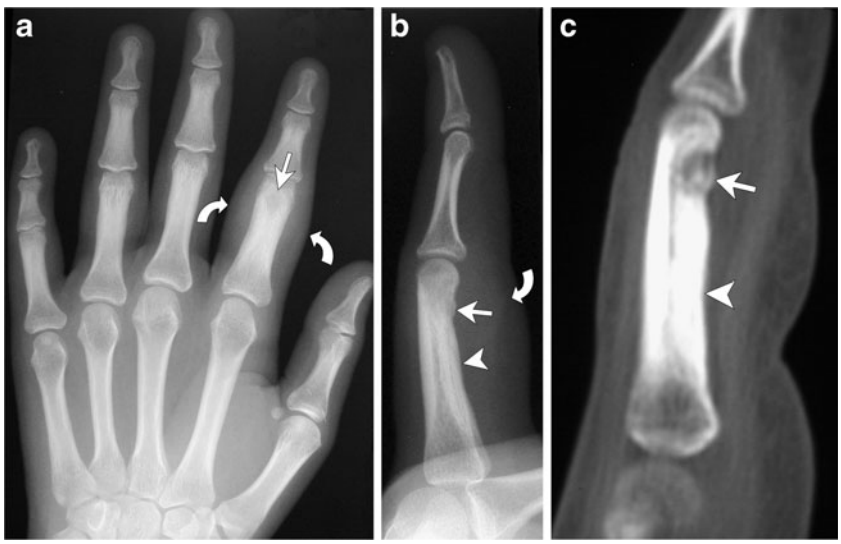

Fig. 11 Osteoid osteoma of the proximal phalanx in a 15-year-old girl with swelling. AP (**a**) and lateral (**b**) radiographs of the hand show a lucent nidus in the second proximal phalanx (*straight arrows*) with surrounding cortical thickening (*arrowhead*) and adjacent fusiform soft-tissue swelling (*curved arrows*). **c** Sagittal CT reformation demonstrates the lucent nidus with central calcification (*arrow*) and thickened sclerotic cortex of the proximal phalanx (*arrowhead*)

Fig. 12 Osteoid osteoma of the fourth proximal phalanx in a 7-year-old girl with swelling. **a** Oblique radiograph of the fourth digit shows marrow expansion of 4th proximal phalanx with a reticular pattern of sclerosis and surrounding soft-tissue swelling. Sagittal STIR (**b**) and coronal T1-weighted MR images (**c**) show increased T2 and decreased T1 signal of the entire 4th proximal phalanx. Postcontrast images showed diffuse enhancement (not shown). Pathology from a biopsy showed a fibrovascular matrix with delicate lacy osteoid production, histology compatible with osteoid osteoma/osteoblastoma. This is a very unusual imaging presentation and the diagnosis was only made by histology

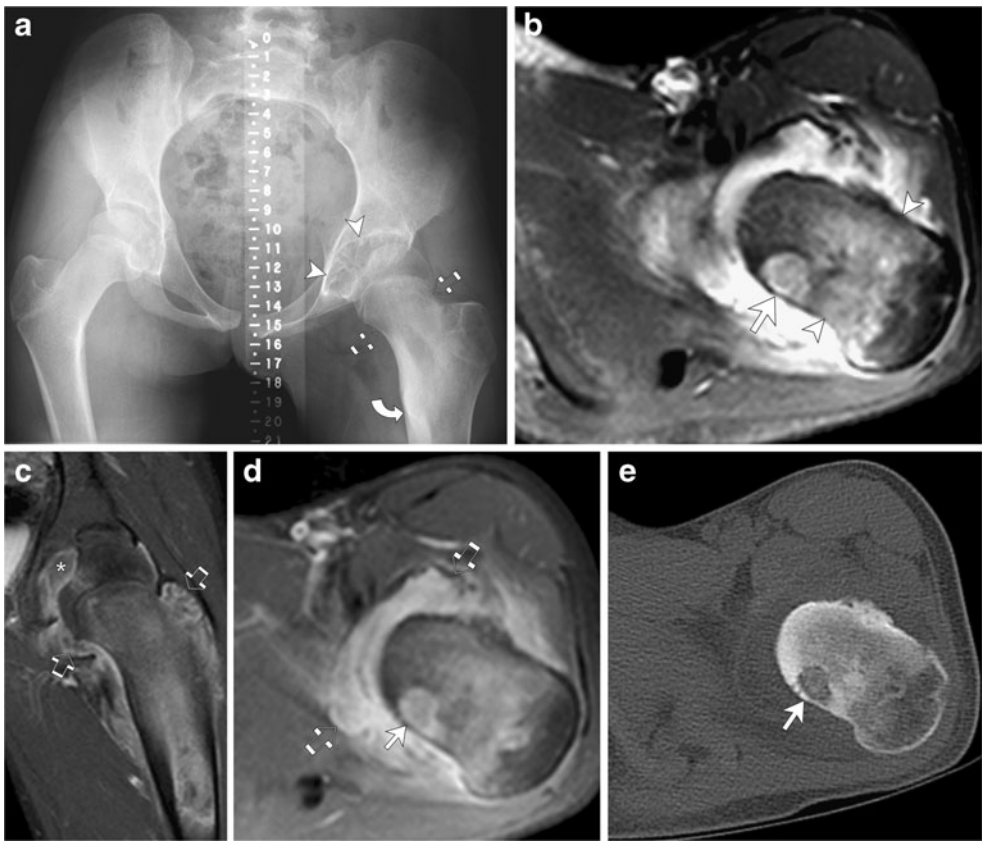

Fig. 13 Intra-articular osteoid osteoma in a 12-year-old girl with leg length discrepancy and hip joint contracture. **a** AP radiograph of the pelvis shows osteopenia of the left proximal femur with shortening and widening of the femoral neck (*straight arrows*). There is medial cortical thickening of the proximal femur (*curved arrow*). The left hip joint is widened with erosive changes of the acetabulum, suggestive of a joint effusion and synovitis (*arrowheads*). There is a 0.7-cm leg length discrepancy, left longer than right. **b** Axial fat-saturated T2-weighted MR image shows a rounded intra-articular nidus (*white arrow*) and proximal femoral marrow edema (*arrowheads*). Coronal (**c**) and axial (**d**) fat-saturated postcontrast T1-weighted MR images show the enhancing nidus (*white arrow*) and enhancing synovitis (*thick arrows*) surrounding the joint effusion (*asterisk*). **e** Axial CT image shows the radiolucent nidus (*arrow*) with faint internal calcifications

regard to the innervation of osteoid osteomas, as the greatest concentration of nerves is found in the reactive zone, which might explain the intense sclerosis at this site [3, 21, 22].

Classification

Osteoid osteomas can be classified based on their location within bone (Fig. 1) [24]. The most common presentation, or "classic" type, is cortical with the radiolucent nidus located in the center of fusiform cortical thickening (Fig. 2). This is usually seen in the diaphysis or metaphysis of long tubular bones, especially the tibia and femur. The value of CT in the diagnosis of osteoid osteoma has been well documented in the literature [25–28]. Although recent literature recommends the use of non-ionizing imaging modalities in children, the role of MRI in diagnosing osteoid osteoma remains controversial, despite recent reports advocating the utility of it for the diagnosis of osteoid osteomas (Fig. 3) [29–31].

Nonetheless, the differentiation of osteoid osteomas from other masses may still be problematic, especially when they occur in less common and atypical locations, such as the subperiosteal space, medullary cavity, spine or non-long bone lesions, or in lesions that have atypical features [25–28].

On CT, the nidus may be lucent or may have central calcifications. The recently described "CT vessel" or "vascular groove" sign is highly specific for osteoid osteomas, and can be seen as curvilinear low-density grooves entering or in proximity to the nidus (Fig. 4) [32, 33]. On MRI, the nidus demonstrates low to intermediate signal intensity on T1-weighted images with enhancement, following intravenous contrast injection. In the authors' experience [34], a rim of low SI on all pulse sequences is often seen surrounding the nidus, which corresponds to the peripheral rim of sclerosis seen on pathology. Adjacent reactive bone marrow and soft-tissue edema appear hyperintense on T2-weighted images and may also demonstrate enhancement after the administration of intravenous contrast agent.

Medullary osteoid osteomas are typically juxta-articular in location, and are often seen in the femoral neck, hands, feet and posterior elements of the spine (Fig. 5). Medullary lesions show mild to moderate reactive sclerosis, which may be remote from the nidus [2].

Subperiosteal lesions are located on the external aspect of the cortex, and are frequently seen along the medial aspect of the femoral neck, hands, feet and neck of the talus (Fig. 6). These lesions cause pressure, atrophy or erosion of the underlying cortical bone and may have less compact periosteal reaction than typical cortical osteoid osteomas. Endosteal osteoid osteomas are located on the internal aspect of the cortex and may cause an atypical cortical circumferential thickening. It has been suggested that cortical, medullary and endosteal lesions migrate from a subperiosteal location [24].

Intra-articular

While not part of the classification described by Kayser et al. [24], intra-articular osteoid osteomas have an atypical presentation and imaging appearance. The clinical symptoms include joint tenderness, stiffness, swelling and

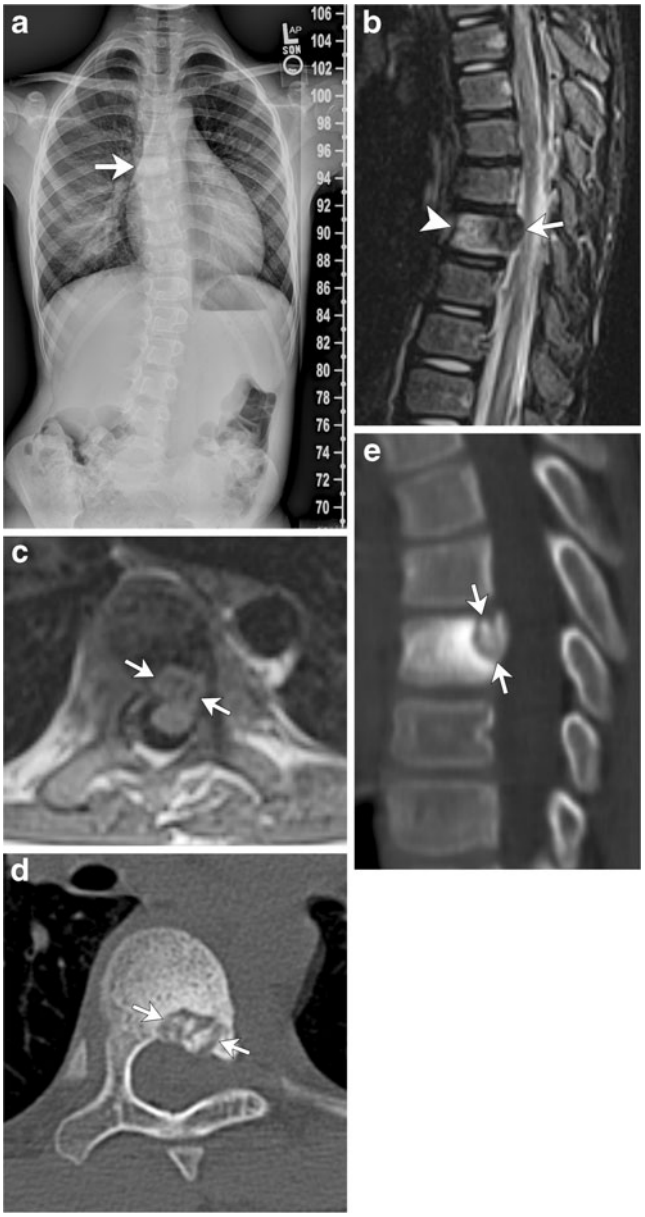

Fig. 14 Spinal osteoid osteoma in an 8-year-old boy with scoliosis. **a** AP radiograph from a scoliosis series shows sclerosis of the T7 vertebral body (*arrow*) with a mild S-shaped scoliosis. The dominant upper thoracic dextrocurvature is centered at T7. Sagittal T2-weighted (**b**) and axial T1-weighted (**c**) MR images demonstrate a T2 hypointense and T1 intermediate signal nidus (*arrows*) in the left posterior aspect of T7 with bone marrow edema (*arrowhead*) within the vertebral body. Axial (**d**) and reformatted sagittal (**e**) CT images show a radiolucent nidus (*arrows*) with irregular central calcification and surrounding sclerosis of the T7 vertebral body

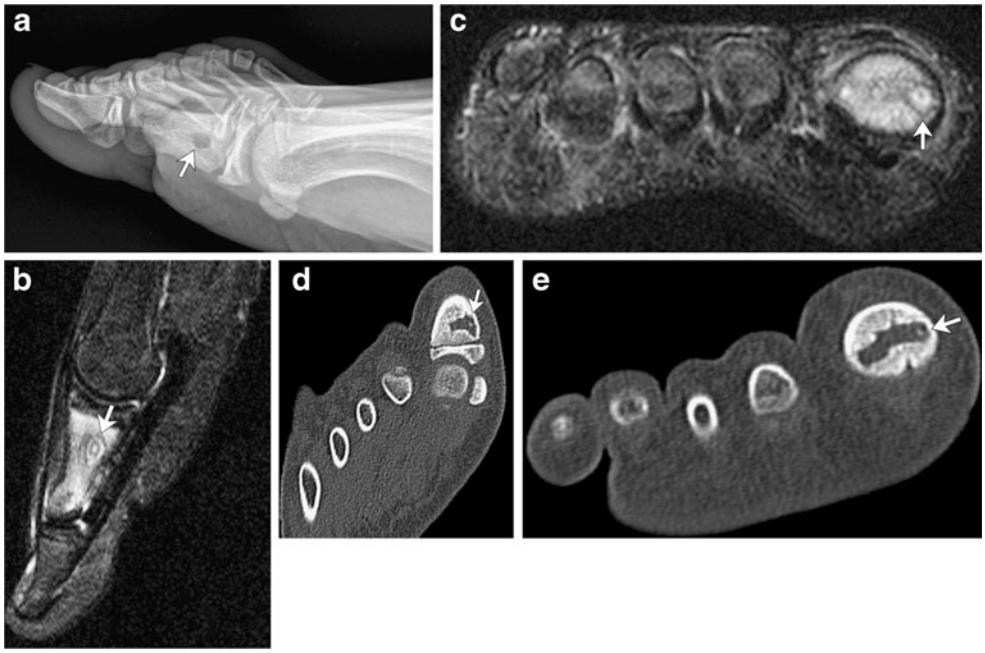

Fig. 15 An 8-year-old boy with great toe pain. **a** Lateral radiograph of the foot shows a circumscribed lucency in the proximal aspect of the first proximal phalanx (*arrow*) without surrounding sclerosis. Sagittal STIR (**b**) and short-axis axial fat-saturated T2-weighted (**c**) MR images demonstrate a rounded T2 hyperintense lesion with hypointense rim (*arrows*) thought to represent a nidus of an osteoid osteoma with surrounding sclerosis. Note high T2 signal of the remainder marrow consistent with edema. Axial (**d**) and coronal reformatted (**e**) CT images show an elongated lucent lesion at the base of the 1st proximal phalanx with a small central calcification medially (*arrow*). This was thought to represent an osteoid osteoma, though infection and Langerhan cell histiocytoma were also considered. Pathology showed small fragments of acellular bone suggestive of sequestrum surrounded by a plasmacytic infiltrate, most consistent with chronic osteomyelitis

effusion, which can mimic infection or arthritis. The pain may not be worse at night. The most frequently affected joint is the hip, with the ankle, elbow, wrist and knee less common [31, 35]. On imaging, there is minimal or absent reactive cortical thickening and sclerosis due to lack of cambium in the inner layer of periosteum (Fig. 7) [4]. There is frequently a reactive joint effusion with a lymphoproliferative synovitis and widening of the joint space [36]. Soft-tissue abnormalities can be observed in up to 50% of patients. Atrophy of adjacent muscles, evidenced by fatty replacement, has also been reported. When involving the proximal femur, extensive bone marrow edema may be appreciated extending from the femoral neck into the proximal diaphysis [31]. If the nidus is not identified, these findings can lead to misdiagnosis of infection or neoplasm (Fig. 8) [31].

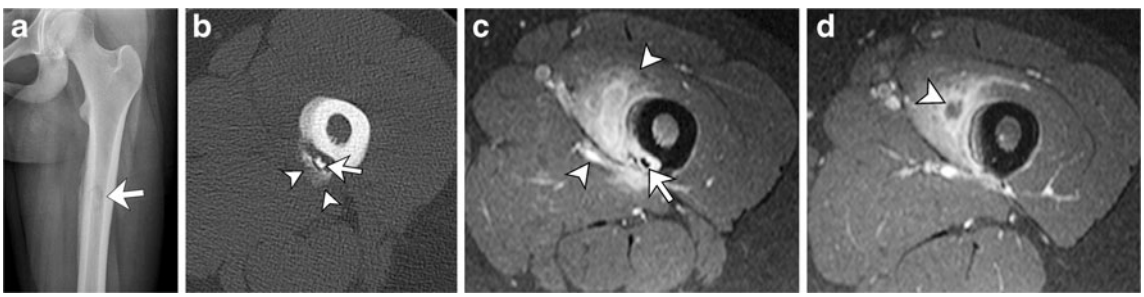

Fig. 16 Images in a 13-year-old girl with 2 weeks of left thigh pain. No fevers and normal inflammatory markers. **a** AP radiograph of the proximal left femur shows thick, wavy periosteal reaction along medial proximal diaphysis. A region of central lucency projects within the medullary canal (*arrow*). **b** Axial CT image shows an ovoid intracortical lucency with irregular borders with central irregular calcification (*arrow*) and periosteal reaction (*arrowheads*). Due to the irregular appearance of the periosteal reaction and atypical appearance for an osteoid osteoma, an MRI was ordered. **c** Axial fat-saturated T1-weighted post-gadolinium MR image shows marked enhancement within the adjacent medial soft tissues (*arrowheads*) as well as surrounding the central calcification within the lesion (*arrow*). There is a mild amount of enhancement within the femur. **d** Axial image more inferiorly shows a small abscess within the medial soft tissues of the thigh (*arrowhead*), highly suspicious for infection. The region was biopsied and the culture was positive for *Staphylococcus aureus*, consistent with osteomyelitis with a sequestrum

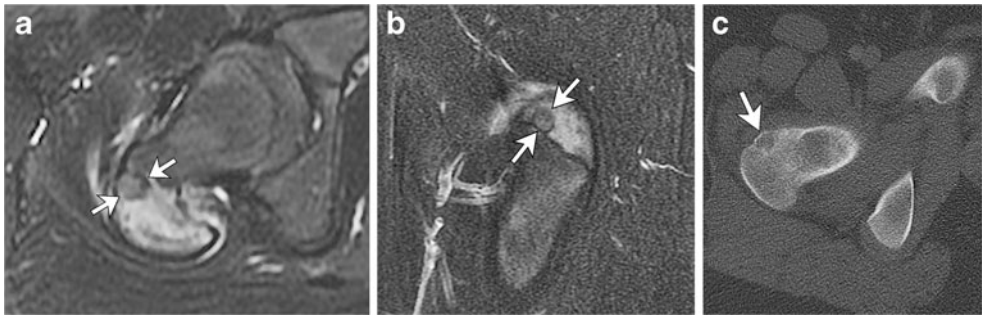

Fig. 17 Images in a 13-year-old boy with right hip pain for 5 months, radiating down the leg. Axial (**a**) and sagittal (**b**) fat-saturated T2-weighted images of the right greater trochanteric apophysis demonstrate marrow edema with a rounded lesion and peripheral hypointensity (*arrows*). There is mild edema within the adjacent soft tissues. As the apophysis is an unusual location for osteoid osteomas, a CT was ordered for further evaluation. **c** Axial CT image demonstrates a rounded lucent lesion with slightly irregular borders and no discrete rim of sclerosis (*arrow*). The borders of the lucency are irregular and there is no central calcification, which is less common for an osteoid osteoma. A chondroblastoma was suspected and confirmed at biopsy

Spine

Spinal osteoid osteomas are more frequently located in the posterior elements (Fig. 9). The lumbar spine is the most common location, followed by the cervical and thoracic spine, and the sacrum. Patients may present with radicular pain, painful scoliosis or gait disturbances. Plain films can show reactive sclerosis, but due to the anatomy and overlapping structures, CT or MRI is usually needed for localization of the lesion [4].

Hands and feet

Carpal and tarsal osteoid osteomas are usually intramedullary and are considered intra-articular in these locations (Fig. 10). There is less reactive sclerosis than a typical cortical lesion and inflammatory changes may involve the adjacent bones, soft tissues and joints, causing synovitis and joint effusion (Fig. 11). Lesions of the tubular bones of the hands and feet are most commonly cortical, and can present with soft-tissue swelling, clinically mimicking infection or arthritis (Fig. 12) [4].

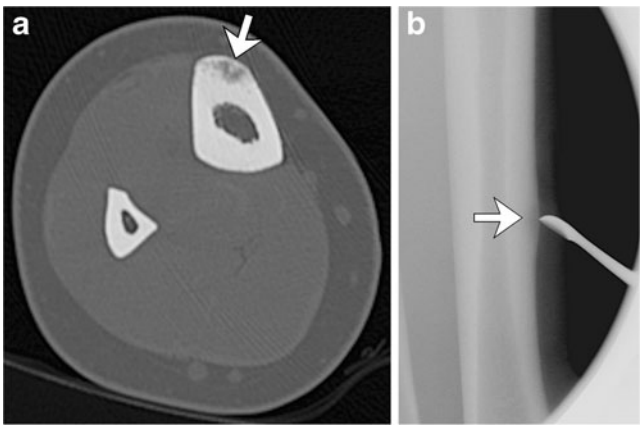

Fig. 18 Images in a 14-year-old girl with painful nodular swelling along the right distal anterior tibia. **a** Axial CT image shows focal rounded lucency with a more central region of sclerosis within the anterior tibial cortex (*arrow*), suggestive of an osteoid osteoma. While the cortex appears focally thickened, there is no overlying fusiform periosteal reaction, as would be expected in an osteoid osteoma. A biopsy was performed. **b** Lateral radiograph during biopsy demonstrates rounded intracortical osteolysis (*arrow*) with thickening of the anterior tibial cortex. Biopsy confirmed osteofibrous dysplasia

Growth disturbances

Osteoid osteomas can cause failure of normal tubulation of long bones, bony overgrowth and disuse osteopenia, resulting in growth disturbances (Fig. 13). When located near a physis, an osteoid osteoma can lead to a leg length discrepancy, elongating the affected limb [22]. Other complications

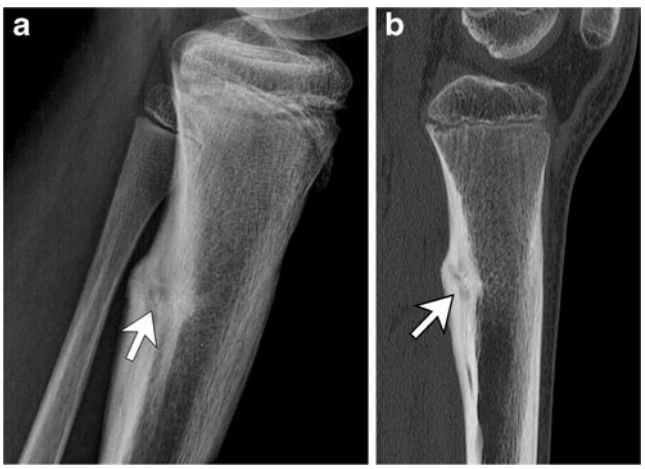

Fig. 19 Images in a 11-year-old boy with right knee pain for 3 weeks and no known trauma. **a** Lateral radiograph of the proximal tibia demonstrates cortical thickening along the posterior diametaphysis with central lucency and a more sclerotic appearance centrally (*arrow*), suggesting an osteoid osteoma. **b** Sagittal CT of the proximal tibial clearly shows a fracture lucency with surrounding callus (*arrow*)

of growth caused by osteoid osteomas include angular deformity, joint contracture and scoliosis with atrophy of the paraspinal muscles (Fig. 14).

Differential considerations

While imaging characteristics of osteoid osteomas can often be straightforward, other lesions can mimic their radiologic appearance. A Brodie abscess of chronic osteomyelitis with a radiolucent center and surrounding reactive sclerosis can appear much like an osteoid osteoma when small in size (Fig. 15). In an intracortical abscess, the sequestrum is often irregular in shape and the inner margin of the area of lucency is not smooth, in contrast to an osteoid osteoma, which often has smooth inner margins (Fig. 16) [4]. Tumors can also pose a diagnostic challenge. Chondroblastomas occur in the epiphyses of children and can appear as an osteolytic lesion associated with extensive bone marrow edema as well as periosteal reaction, similar to an osteoid osteoma. An epiphyseal and intramedullary location can help differentiate chondroblastomas from osteoid osteomas, which the latter are more commonly diaphyseal and intracortical (Fig. 17) [4, 37]. In children, cortical tibial lesions require special consideration because a variety of pathologies within the cortex of the tibia can produce cortical thickening and proliferation, such as osteofibrous dysplasia (Fig. 18), adamantinoma and stress fractures [38]. Stress fractures, commonly seen within the lower extremities, can mimic osteoid osteomas on conventional radiography, as both can produce focal cortical thickening of varying degrees. Cross-sectional imaging is helpful to delineate a discrete fracture line in an area of cortical thickening, as opposed to the central nidus of an osteoid osteoma (Fig. 19).

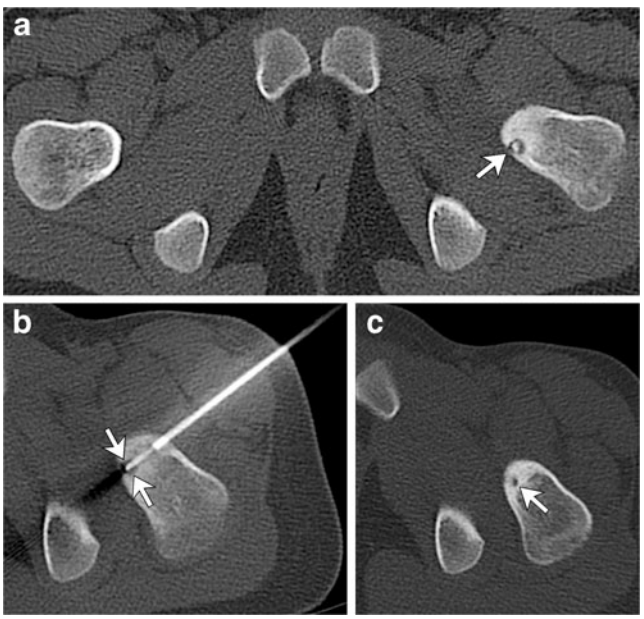

Fig. 20 Treatment failure in a 7-year-old girl with hip pain. **a** Initial axial CT obtained after 4 months of hip pain, which was relieved by aspirin. There is central rounded lucency within the posterior left femoral neck that contains a calcified nidus consistent with an osteoid osteoma (*arrow*). **b** Axial CT image during radiofrequency ablation shows proper positioning of the electrode tip within the nidus (*arrows*). **c** Follow-up CT obtained 7 months after treatment for persistent hip pain shows residual rounded lucency within the femoral neck (*arrow*). The girl had a second radiofrequency ablation and has been symptom-free

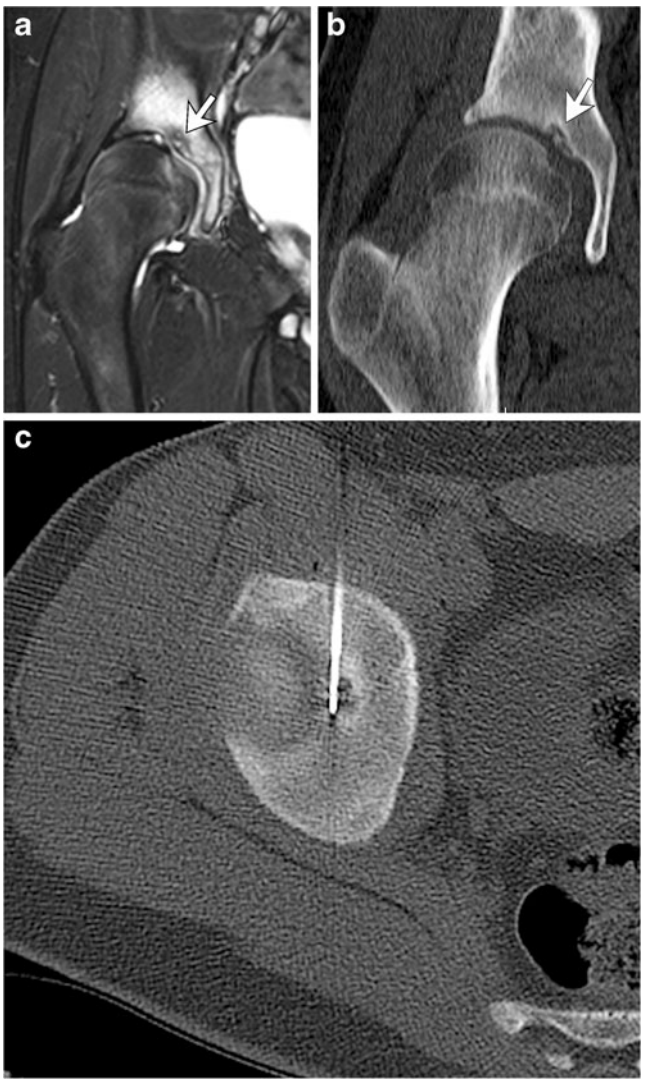

Fig. 21 Osteoid osteoma within the right acetabular roof in a 13-year-old boy with 2 months of right hip and thigh pain. Hip contracture on examination. **a** Coronal fat-saturation T2 image of the right hip shows extensive edema within the right acetabulum with a focal lesion within the right acetabular roof with surrounding hypointense rim (*arrow*), suggesting an osteoid osteoma. Noted is a small joint effusion. **b** Coronal reformatted CT image shows the lucent lesion within the acetabular roof with a central nidus and thin rim of sclerosis (*arrow*). This lesion is surgically inaccessible and radiofrequency ablation is the preferred treatment option. **c** Axial CT image during radiofrequency ablation demonstrates placement of the electrode tip within the lesion, which is in close proximity to the acetabular articular cartilage

Treatment

Although there is some evidence to suggest that osteoid osteomas may regress spontaneously, this may take several years of observation and pain management with nonsteroidal anti-inflammatory medication, and thus is not a suitable option for children [39, 40]. Complete surgical resection has proved to be curative when the nidus is removed; however, when this approach is used in the weight-bearing bones, a prolonged period of restricted activities may be required. In addition, the surgically created bone defect may lead to pathologic fracture [41]. CT-guided percutaneous resection, a less invasive method, is performed with CT guidance to minimize the amount of excised bone and ensure that the entire nidus is resected, as incomplete resection can lead to recurrence. At our institution, surgically resected osteoid osteomas are all performed with CT guidance, with 40% of children requiring an overnight hospital stay for pain management. When the lower extremities are involved, activities are restricted to toe touch weight-bearing for approximately 4 weeks, with slow progression to full weight-bearing over the next 4 weeks.

Radiofrequency (RF) ablation has been successfully used to treat osteoid osteomas for more than 20 years [42] and is currently the choice of treatment for most lesions [41]. RF ablation is performed with the use of CT guidance, and the entire procedure generally takes 90 min to perform. The RF electrode is inserted with the tip directed toward the nidus and thermal heating is applied for 4–6 min. Larger lesions may require multiple ablation cycles with repositioning of the electrode tip. Success rates have been reported as high as 90% (Fig. 20) [41]. RF is preferred over a surgical approach in treating epiphyseal lesions that may require arthrotomy with resultant impairment of bone growth and/or joint mobility. Intra-articular lesions, located on or immediately beneath joint surfaces, adjacent to the articular cartilage have also successfully been treated with RF ablation and have been well tolerated (Fig. 21) [39]. Percutaneous RF ablation may not be advisable for spinal osteoid osteomas or lesions within the hand, as the cortex may not be a reliable insulator to protect the adjacent neural tissue. In our experience, patients treated with RF ablation are discharged to home the same day and very few require pain medications. All daily activities are resumed immediately and there are no restricted activities.

Conclusion

In most cases, the classic appearance of an osteoid osteoma does not pose a diagnostic challenge. Throbbing pain at night that responds to salicylates and the radiolucent nidus surrounded by variable degrees of reactive sclerosis are distinctive features of osteoid osteomas that usually lead to a straightforward diagnosis. However, on occasion, the clinical picture and the imaging findings are atypical and may lead to difficulties in diagnosis. Lesions in atypical locations can have a confusing clinical presentation and appearance on MR imaging. Incorrect diagnosis may delay treatment, which can result in long-term morbidity, especially with intra-articular lesions. Knowledge of these atypical findings should lead to a careful search for a nidus, prompting a subsequent CT. Mimics of osteoid osteoma should be considered in the differential diagnosis, as imaging appearances can have overlapping findings. Radiologists should be familiar with these less common forms of osteoid osteoma to avoid extensive workups, unnecessary invasive procedures and delayed treatment.

Acknowledgements This work was awarded an honorable mention as an educational poster at SPR 2012, San Francisco, CA.

We thank Dr. Anne Marie Cahill from the Department of Radiology and Dr. John Dormans from the Department of Orthopedics at the Children's Hospital of Philadelphia for their help and contributions to this manuscript.

References

1. Jaffe HL (1935) Osteoid osteoma: a benign osteoblastic tumor composed of osteoid and atypical bone. Arch Surg 31:709–728
2. Kransdorf MJ, Stull MA, Gilkey FW et al (1991) Osteoid osteoma. Radiographics 11:671–696
3. Iyer RS, Chapman T, Chew FS (2012) Pediatric bone imaging: diagnostic imaging of osteoid osteoma. AJR 198:1039–1052
4. Chai JW, Hong SH, Choi J-Y et al (2010) Radiologic diagnosis of osteoid osteoma: from simple to challenging findings. Radiographics 30:737–749, Erratum appears in Radiographics [2010] 30:1156
5. Swee RG, McLeod RA, Beabout JW (1979) Osteoid osteoma. Detection, diagnosis, and localization. Radiology 130:117–123
6. Lindbom A, Lindvall N, Soderberg G et al (1960) Angiography in osteoid osteoma. Acta Radiol 54:327–333
7. Helms CA, Hattner RS, Vogler JB 3rd (1984) Osteoid osteoma: radionuclide diagnosis. Radiology 151:779–784
8. Gil S, Marco SF, Arenas J et al (1999) Doppler duplex color localization of osteoid osteomas. Skeletal Radiol 28:107–110
9. Ebrahim FS, Jacobson JA, Lin J et al (2001) Intraarticular osteoid osteoma: sonographic findings in three patients with radiographic, CT, and MR imaging correlation. AJR 177:1391–1395
10. von Kalle T, Langendörfer M, Fernandez FF et al (2009) Combined dynamic contrast-enhancement and serial 3D-subtraction analysis in magnetic resonance imaging of osteoid osteomas. Eur Radiol 19:2508–2517
11. Mungo DV, Zhang X, O'Keefe RJ et al (2002) COX-1 and COX-2 expression in osteoid osteomas. J Orthop Res 20:159–162
12. Greco F, Tamburrelli F, Ciabattoni G (1991) Prostaglandins in osteoid osteoma. Int Orthop 15:35–37
13. Kawaguchi Y, Sato C, Hasegawa T et al (2000) Intraarticular osteoid osteoma associated with synovitis: a possible role of cyclosteoid osteomaxygenase-2 expression by osteoblasts in the nidus. Mod Pathol 13:1086–1091
14. Kawaguchi Y, Hasegawa T, Oka S et al (2001) Mechanism of intramedullary high intensity area on T2-weighted magnetic

resonance imaging in osteoid osteoma: a possible role of COX-2 expression. Pathol Int 51:933–937
15. Yamamura S, Sato K, Sugiura H et al (1997) Prostaglandin levels of primary bone tumor tissues correlate with peritumoral edema demonstrated by magnetic resonance imaging. Cancer 79:255–261
16. Ehara S, Rosenthal DI, Aoki J et al (1999) Peritumoral edema in osteoid osteoma on magnetic resonance imaging. Skeletal Radiol 28:265–270
17. Ekmekci P, Bostanci S, Erdogan N et al (2001) A painless subungual osteoid osteoma. Dermatol Surg 27:764–765
18. Basu S, Basu P, Dowell JK (1999) Painless osteoid osteoma in a metacarpal. J Hand Surg (Br) 24:133–134
19. Lee EH, Shafi M, Hui JHP (2006) Osteoid osteoma: a current review. J Pediatr Orthop 26:695–700
20. Kneisl JS, Simon MA (1992) Medical management compared with operative treatment for osteoid-osteoma. J Bone Joint Surg Am 74:179–185
21. O'Connell JX, Nanthakumar SS, Nielsen GP et al (1998) Osteoid osteoma: the uniquely innervated bone tumor. Mod Pathol 11:175–180
22. Hasegawa T, Hirose T, Sakamoto R et al (1993) Mechanism of pain in osteoid osteomas: an immunohistochemical study. Histopathology 22:487–491
23. Hukkanen M, Konttinen YT, Santavirta S et al (1993) Rapid proliferation of calcitonin gene-related peptide-immunoreactive nerves during healing of rat tibial fracture suggests neural involvement in bone growth and remodelling. Neuroscience 54:969–979
24. Kayser F, Resnick D, Haghighi P et al (1998) Evidence of the subperiosteal origin of osteoid osteomas in tubular bones: analysis by CT and MR imaging. AJR 170:609–614
25. Hayes CW, Conway WF, Sundaram M (1992) Misleading aggressive MR imaging appearance of some benign musculoskeletal lesions. Radiographics 12:1119–1134, discussion 1135–1136
26. Hosalkar HS, Garg S, Moroz L et al (2005) The diagnostic accuracy of MRI versus CT imaging for osteoid osteoma in children. Clin Orthop Relat Res 171–177
27. Lefton DR, Torrisi JM, Haller JO (2001) Vertebral osteoid osteoma masquerading as a malignant bone or soft-tissue tumor on MRI. Pediatr Radiol 31:72–75
28. Assoun J, Richardi G, Railhac JJ et al (1994) Osteoid osteoma: MR imaging versus CT. Radiology 191:217–223
29. Spouge AR, Thain LM (2000) Osteoid osteoma: MR imaging revisited. Clin Imaging 24:19–27
30. Liu PT, Chivers FS, Roberts CC et al (2003) Imaging of osteoid osteoma with dynamic gadolinium-enhanced MR imaging. Radiology 227:691–700
31. Gaeta M, Minutoli F, Pandolfo I et al (2004) Magnetic resonance imaging findings of osteoid osteoma of the proximal femur. Eur Radiol 14:1582–1589
32. Liu PT, Kujak JL, Roberts CC et al (2011) The vascular grosteoid osteomave sign: a new CT finding associated with osteoid osteomas. AJR 196:168–173
33. Yaniv G, Shabshin N, Sharon M et al (2011) Osteoid osteoma—the CT vessel sign. Skeletal Radiol 40:1311–1314
34. Epelman M, Jaramillo D, Hosalkar HS et al (2008) Usefulness of the "hypointense halo sign" in the MRI diagnosis of osteoid osteoma. Pediatr Radiol 38(Suppl 2):S296
35. Allen SD, Saifuddin A (2003) Imaging of intra-articular osteoid osteoma. Clin Radiol 58:845–852
36. Snarr JW, Abell MR, Martel W (1973) Lymphofollicular synovitis with osteoid osteoma. Radiology 106:557–560
37. Hudson TM, Hawkins IF (1981) Radiologic evaluation of chondroblastoma. Radiology 139:1–10
38. Levine SM, Lambiase RE, Petchprapa CN (2003) Cortical lesions of the tibia. Radiographics 23:157–177
39. Rosenthal DI, Hornicek FJ, Torriani M et al (2003) Osteoid osteoma: percutaneous treatment with radiofrequency energy. Radiology 229:171–175
40. Shinozaki T, Sato J, Watanabe H et al (2005) Osteoid osteoma treated with computed tomography-guided percuteneous radiofrequency ablation: a case series. J Orthop Surg 13:317–322
41. Montamedi D, Learch TJ, Ishimitsu DN et al (2009) Thermal ablation of osteoid osteoma: overview and step-by-step guide. Radiographics 29:2127–2141
42. Tillotson CL, Rosenberg AE, Rosenthal DI (1989) Controlled thermal injury of bone: report of a percutaneous technique using radiofrequency electrode and generator. Invest Radiol 24:888–892